

Title	Microstructure and nanomechanical properties of cubic boron nitride films prepared by bias sputter deposition
Author(s)	Yamada, Yukiko; Tsuda, Osamu; Yoshida, Toyonobu
Citation	Thin Solid Films, 316(1-2): 35-39
Issue Date	1998-03-21
Type	Journal Article
Text version	author
URL	<a href="http://hdl.handle.net/10119/4969">http://hdl.handle.net/10119/4969</a>
Rights	NOTICE: This is the author's version of a work accepted for publication by Elsevier. Yukiko Yamada, Osamu Tsuda and Toyonobu Yoshida, Thin Solid Films, 316(1-2), 1998, 35-39, <a href="http://dx.doi.org/10.1016/S0040-6090(98)00384-8">http://dx.doi.org/10.1016/S0040-6090(98)00384-8</a>
Description	



Published in Thin Solid Films 316, 35-39 (1998).

Microstructure and nanomechanical properties of cubic boron nitride films prepared by bias sputter deposition

Yukiko Yamada\*, Osamu Tsuda and Toyonobu Yoshida

Department of Metallurgy and Materials Science, Graduate School and Faculty of Engineering, The University of Tokyo, 7-3-1 Hongo Bunkyo-ku Tokyo 113 Japan.

\*Research Fellow of Japan Society for the Promotion of Science,  
e-mail:yukiko@plasma.t.u-tokyo.ac.jp

Abstract

Nanoindentations, using a triangular based cube-corner shaped diamond tip, were tried to study the mechanical properties of cubic boron nitride (*c*BN) films. Since the *c*BN film has a layered structure consisting of an initial  $sp^2$ -bonded BN (amorphous BN and turbostratic BN) layer and a  $sp^3$ -bonded BN (*c*BN) layer, which was previously studied by cross-sectional transmission electron microscopy (TEM), *c*BN films in different growth stages were prepared for the measurements. Hardness and elastic modulus were evaluated as a function of the penetration depth from the obtained loading-unloading curves using a method described by Oliver *et al.* The maximum hardness and elastic modulus of a 110-nm-thick *c*BN film (including an approximately 50-nm-thick initial layer) were approximately 10 and 3 times, respectively, larger than the values evaluated for a silicon wafer substrate. The dependence of the evaluated hardness and the elastic modulus on film thickness and penetration depth can be explained in

terms of the layered structure of the *c*BN film, i. e. soft initial  $sp^2$ -bonded BN layer with low elastic modulus, and hard *c*BN layer with high elastic modulus.

## 1. Introduction

*c*BN is known as the second hardest material next to diamond, which makes it a promising material for hard coating. *c*BN films have been synthesized by various ion-assisted vapor deposition methods[1]. The obtained *c*BN films were polycrystalline and nanocrystalline, so the film surface was smooth in the nanometer range[2], which makes these films suitable for tribological use. The vapor deposited *c*BN films exhibited extreme hardness such as 4000 kg/mm<sup>2</sup> as obtained by the micro-Vickers hardness measurement[3], 42.2 to 61.8 GPa for the Knoop hardness measurement (load 100 mN)[4], and 57.6 GPa for ultra low load indentation (load 10 mN)[5]. The reported friction and wear properties of *c*BN films were better than those of *h*BN films and *a*BN films[6][7]. Since the *c*BN films have a limited film thickness of about a few 100 nm due to delamination from the substrates caused by high compressive film stress and poor adhesion, the measurement of hardness by the conventional indentation method without substrate effect is very difficult. What makes it more complex is that a layered structure of the *c*BN films consists of initial non-*c*BN and *c*BN layers. Nanoindentations with an extremely low load, a highly sharp tip and an extremely shallow penetration depth along with additional structural analyses are necessary to study the mechanical properties of such films.

In this study, nanoindentations using a cube-corner shaped diamond tip were tried to study the mechanical properties of *c*BN films. To study the effects of the layered structure on the mechanical properties, *c*BN films in different growth stages were examined. The dependence of evaluated hardness and elastic modulus on film thickness and penetration depth were discussed in correlation with the layered structure of the *c*BN films.

## 2. Experimental

*c*BN films were deposited on p-type  $\langle 100 \rangle$  oriented silicon wafers by RF bias sputter deposition. The detailed descriptions of our apparatus are reported elsewhere[8]. A sintered *h*BN disc (Shin-Etsu Kagaku, KD-3S) was used as a sputtering target, and Ar was used as a sputtering gas with the pressure of 16 mTorr. The target input RF power was 600 W, and the substrate input RF power was feedback controlled so that the negative substrate bias voltage was constant at 300 V. All depositions were carried out after presputtering the target and substrate for 15 min., with the shutters between the electrodes closed. The deposition condition was maintained constant for all depositions except for deposition time  $t$  ranging from 45 s to 300 s. The maximum thickness of the films measured from a cross-sectional scanning electron microscope (SEM) image was approximately 110 nm, and all the films adhered to the substrates during the measurements. The detail results of the characterization of the films by Fourier transform infrared spectroscopy and X-ray photoelectron spectroscopy are reported elsewhere[9]. The films were characterized as follows. The films in the initial layer growth stage ( $t = 45 \text{ s} \sim 60 \text{ s}$ ) consisted of only *a*BN or *t*BN. The films in the transition stage ( $t = 75 \text{ s} \sim 90 \text{ s}$ ) contained *c*BN on the film surface but *t*BN was also present and the surface was not completely covered with *c*BN. The surface of the films in the cubic layer growth stage ( $t = 120 \text{ s} \sim 300 \text{ s}$ ) were completely covered with *c*BN and the *c*BN layer thickness increased with the deposition time.

Nanoindentations were carried out with a transducer (Triboscope, Hysitron) equipped AFM (Nanoscope III, Digital Instruments) under ambient conditions.

Surface imagings and indentations were performed with the same tip. Indenting locations were carefully chosen by surface imagings so that the indents were always made at fresh places with no irregular deposits. A diamond tip with a triangular based cube-corner shape was mainly used in this study. It had a half angle of 35.2 degrees and a total included angle of 90 degrees. The tip was acute compared to the commonly-used Berkovich tip which has a half angle of 65.3 degrees and a total included angle of 142.2 degrees. The cube-corner tip penetrated deep into the specimen and induced plastic deformation with a very low load compared to the Berkovich tip because of its tip geometry. The hardness and elastic modulus were evaluated from the loading-unloading curves by the method described by Oliver *et al.* [10]. Since Poisson's ratio for the film was unknown, the elastic modulus were evaluated in the form of  $E/(1-\nu^2)$ . The elastic modulus (76.2 GPa) and Poisson's ratio (0.14) for a quartz glass (T-1030, Toshiba Ceramics) was used for contact area calibration. Maximum loads were varied from 5  $\mu\text{N}$  to 400  $\mu\text{N}$  and the loading rate was set constant at 2  $\mu\text{N/s}$ .

### 3. Results and Discussions

Fig. 1 shows the AFM images of residual indentations obtained after a series of indentations with three different maximum loads (30  $\mu\text{N}$ , 100  $\mu\text{N}$ , 300  $\mu\text{N}$ ) to a silicon wafer and the *c*BN films in different growth stages. The z range of the images is set narrow so that the shape of residual indentations will be clearly shown. Surface roughening due to the film growth was also observed, which is published elsewhere in detail[9]. For the silicon wafer, the residual indentations were observed for indentation with a maximum load as low as 5  $\mu\text{N}$ , and pile-ups were observed. The area of residual indentations decreased as the *c*BN film grew

thick, which indicates the increase in hardness of the specimen by *c*BN film coating. For specimens with only an initial layer, the indents were comparable with those of the silicon wafer, but the pile-ups were smaller. For specimens with a thick *c*BN layer, the area of residual indentations decreased drastically and indentations with low maximum loads did not result in any residual indentations.

Fig. 2 shows the loading-unloading curves obtained for a silicon wafer and the *c*BN films in different growth stages by indentations with a constant maximum load of 100  $\mu$ N. The decrease in the penetration depth was not monotonic against *c*BN film growth. The decrease was slight for films in the initial layer growth stage and the transition stage, but for films in the cubic layer growth stage, there was a substantial decrease in the penetration depth. It is apparent from the curves that the deformations of the films as a result of the indentations changed from partly elastic to completely elastic deformations as the *c*BN layer grew thick. The degree of elastic recovery defined as the elastic deformation depth divided by the total deformation depth increased from 0.4 (silicon wafer,  $t = 0$  s) to 1.0 ( $t = 300$  s) in this series of indentations. Circular residual indentations at a low maximum load in Fig. 1 suggest that the tip was not completely sharp and had a finite radius. The tip radius can be estimated from the load curve of elastic indentation[11]. Assuming that the reduced elastic modulus is 200  $\sim$  400 GPa for the thickest *c*BN film ( $t = 300$  s), the tip radius could be estimated as approximately 12  $\sim$  50 nm from the curve in Fig. 2, which is comparable to the crystal size of *c*BN observed in the TEM study.

Fig. 3 (a) shows the contact depth dependence of the normalized hardness of the *c*BN films evaluated from the loading-unloading curves with various maximum loads. The hardness was normalized with 12 GPa, which was the

evaluated hardness of the silicon substrate in the large penetration depth region. Fig. 3 (b) shows the normalized hardness evaluated at a constant contact depth of  $15 \pm 3$  nm for *c*BN films in different growth stages. The normalized hardness increased slightly for the *c*BN films in the initial layer growth stage, and increased almost linearly as *c*BN formed (transition stage) and grew in single phase (cubic layer growth stage). The normalized hardness of the *c*BN films in the cubic layer growth stage was highly dependent on the contact depth. This dependence on the penetration depth is due to the substrate effect, and the evaluated hardness is not the hardness of film alone since saturation of the hardness was not observed in the small penetration depth region. The hardness of thick *c*BN films was affected by a soft substrate and a soft initial *sp*<sup>2</sup>-bonded layer comprising about half of the 110-nm-thick *c*BN film ( $t = 300$  s) which was previously observed in the TEM image[12]. Therefore the evaluated hardness is the underestimated combination hardness.

Fig. 4 (a) shows the contact depth dependence of the normalized elastic modulus. The elastic modulus was normalized with 170 GPa, which was the evaluated elastic modulus of the silicon wafer at the large penetration depth region. Fig. 4 (b) shows the normalized elastic modulus evaluated at a constant contact depth of  $15 \pm 3$  nm for *c*BN films in different growth stages. The evaluated elastic modulus decreased as the initial layer grew, which reflected the low elastic modulus of *sp*<sup>2</sup>-bonded BN compared to that of the silicon wafer substrate. The elastic modulus increased almost linearly as the *c*BN layer formed and grew. The penetration depth dependence of the evaluated value was also obvious for thick *c*BN films in the cubic layer growth stage, similar to the case of the hardness. The saturation of the elastic modulus at small penetration depth



region was not observed, so the evaluated elastic modulus of *c*BN film was also an underestimated combination value.

#### 4. Conclusion

Nanoindentations were carried out in order to study the mechanical properties of *c*BN films deposited on a silicon wafer by bias sputter deposition. The *c*BN films consisted of an initial  $sp^2$ -bonded BN layer and *c*BN layer, which differ largely in the hardness and elastic modulus. The *c*BN layer exhibited extreme hardness and a high elastic modulus, which were respectively, 10 and 3 times larger than the values evaluated for a silicon wafer, at maximum, and these values are considered to be underestimated. The initial  $sp^2$ -bonded BN layer was slightly harder than a silicon wafer, but the elastic modulus was lower than that of a silicon wafer. A thin ( $\sim 50$  nm) *c*BN layer resulted in a large improvement in the hardness and elastic modulus of the specimen. The bias sputter deposited *c*BN films would be useful for obtaining an ultrathin hard and tribological coating, but the thickness of the initial layer and its effects on the film properties should always be considered and controlled. Due to the small thickness of the films and the layered structure of the *c*BN films, the evaluated hardness and elastic modulus changed with the film thickness and the penetration depth. The measurements of the mechanical properties of *c*BN films must be done carefully, considering the thickness of both the initial layer and the *c*BN layer.

#### Acknowledgment

This work is financially supported by Grant-in-Aid for Scientific Research (A) (No.08405047) and Grant-in-Aid for JSPS Fellows, The Ministry of Education,

Science, Sports and Culture, Japan.

## References

- [1] T. Yoshida, *Diamond and Related Materials*, 5 (1996) 501
- [2] T. Ichiki, S. Amagi and T. Yoshida, *J. Appl. Phys.*, 79 (1996) 4381
- [3] K. Inagawa, K. Watanabe, H. Ohson, K. Saitoh and A. Itoh, *J. Vac. Sci. Technol. A*5 (1987) 2696
- [4] M. Murakawa and S. Watanabe, *Surf. Coat. Technol.* 43/44 (1990) 128
- [5] D. R. McKenzie, *J. Vac. Sci. Technol. B* 11 (1993) 1928
- [6] Shuichi Watanabe, Shojiro Miyake and Masao Murakawa, *Surf. Coat. Technol.* 49 (1991) 406
- [7] S. Miyake, S. Watanabe, M. Murakawa, R. Kaneko and T. Miyamoto, *Thin Solid Films*, 212 (1992) 262
- [8] O. Tsuda, Y. Yamada, T. Fujii and T. Yoshida, *J. Vac. Sci. & Technol.*, A13 (1995) 2843
- [9] Y. Yamada, Y. Tatebayashi, O. Tsuda and T. Yoshida, *Thin Solid Films*, 295 (1997) 137
- [10] W. C. Oliver and G. M. Pharr, *J. Mater. Res.*, 7 (1992) 1564
- [11] K. L. Johnson, Contact mechanics, Cambridge University Press, First paperback edn., 1987, p. 93
- [12] Y. Yamada, Y. Tatebayashi, O. Tsuda and T. Yoshida, *Proceedings of 13th International Symposium of Plasma Chemistry (1997)* in the press

## Figure captions

Fig. 1 AFM images of the residual indentations observed on a silicon wafer and the cBN films in different growth stages. The BN films were in the following growth stages. 0 s : silicon substrate, 60 s : initial layer growth stage, 90 s : transition stage, 150s and 300s : cubic layer growth stage.

Fig. 2 Loading-unloading curves of the cBN films in different growth stages. The maximum load was 100  $\mu$ N. The BN films were in the following growth stages. 0 s : silicon substrate, 45s and 60 s : initial layer growth stage, 75 s and 90 s : transition stage, 150s  $\sim$  300s : cubic layer growth stage.

Fig. 3 (a) Contact depth dependent normalized hardness of cBN films in different growth stages. The hardness was normalized with 12 GPa, which was the hardness of a silicon wafer at the large penetration depth region. The BN films were in the following growth stages. ● : cubic layer growth stage, ▲ : transition stage, ■ : initial layer growth stage, + : silicon substrate.

Fig. 3 (b) Deposition time dependent normalized hardness evaluated at contact depths of  $15 \pm 3$  nm.

Fig. 4 (a) Contact depth dependent normalized elastic modulus of cBN films in different growth stages. Elastic modulus  $E/(1-\nu^2)$  was normalized with 170 GPa, which was the elastic modulus of a silicon wafer at the large penetration depth region. The BN films were in the following growth stages. ● : cubic layer growth stage, ▲ : transition stage, ■ : initial layer growth stage, + : silicon substrate.

Fig. 4 (b) Deposition time dependent normalized elastic modulus evaluated at contact depths of  $15 \pm 3$  nm.



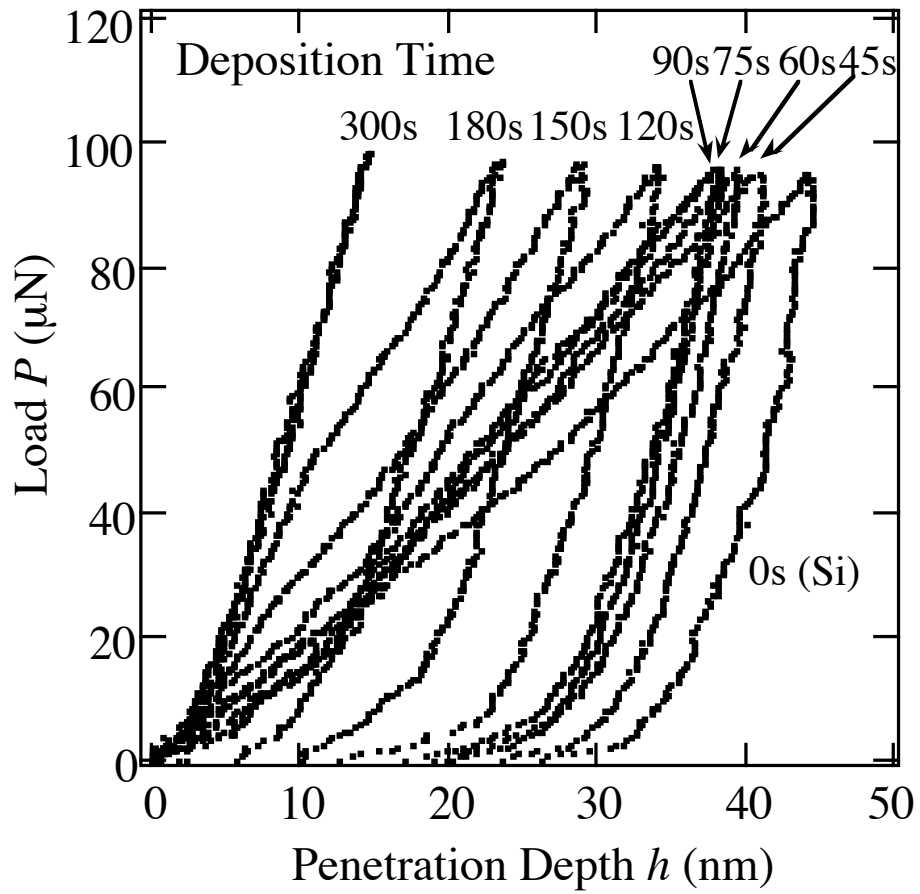


Figure 2

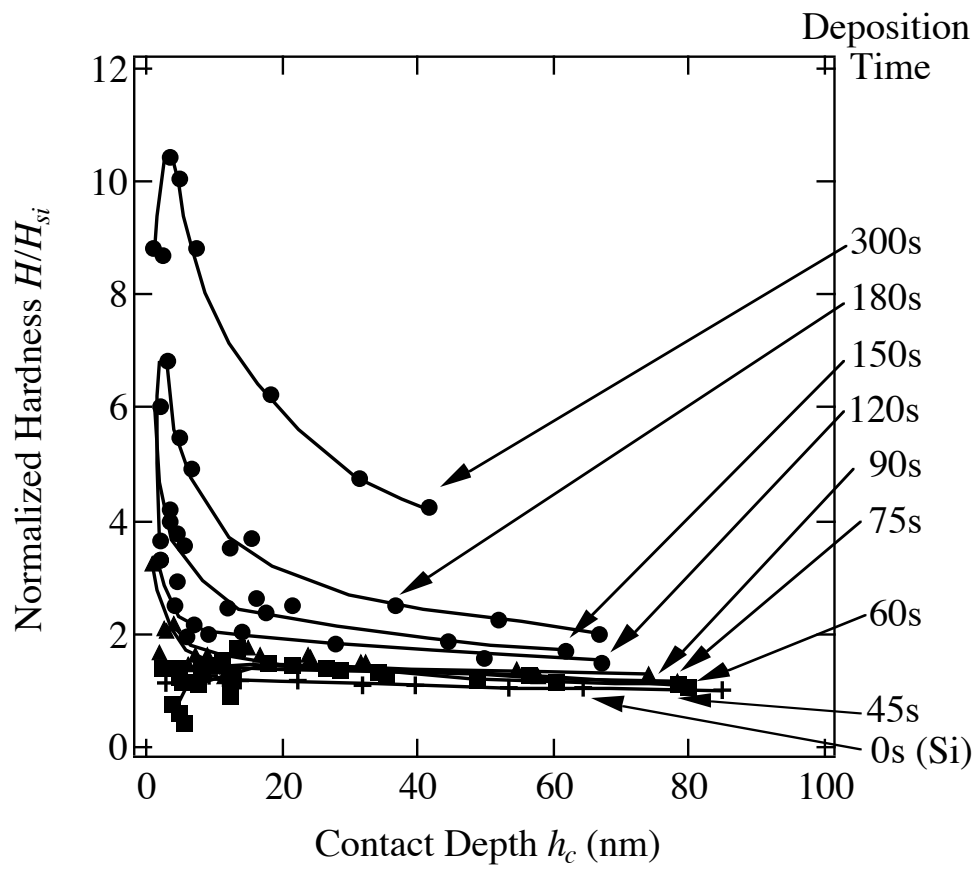


Figure 3 (a)

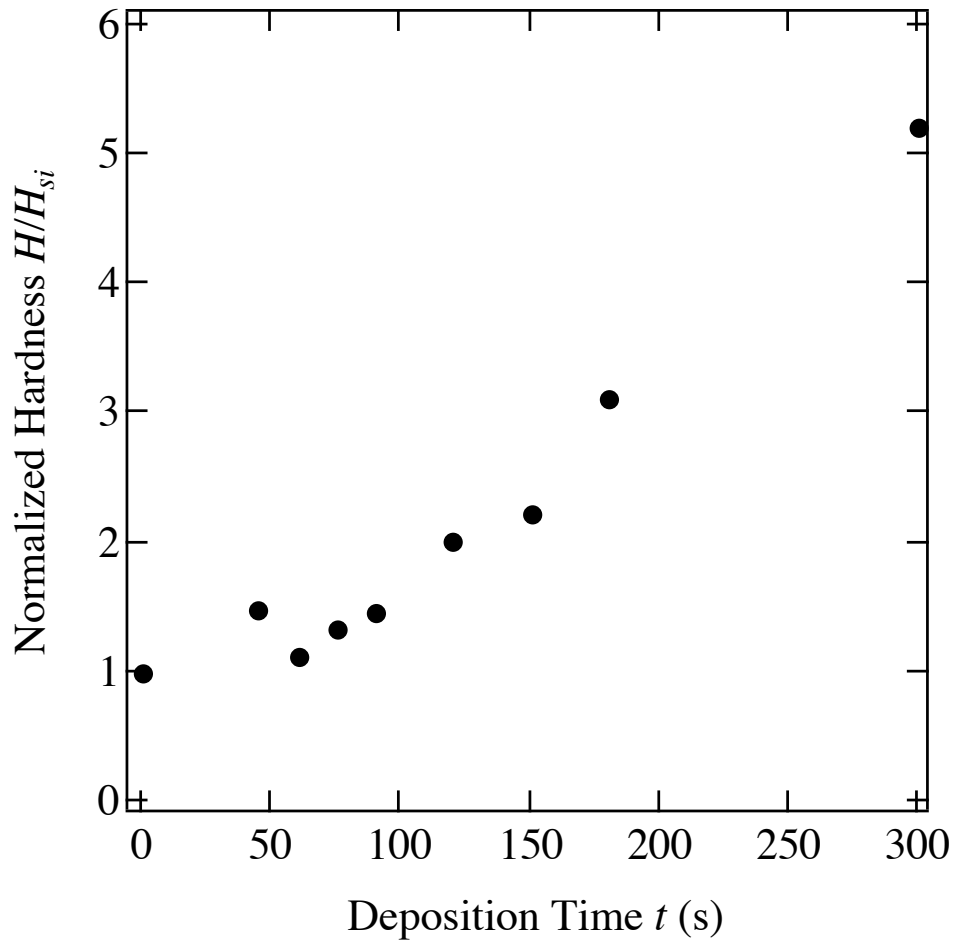


Figure 3 (b)



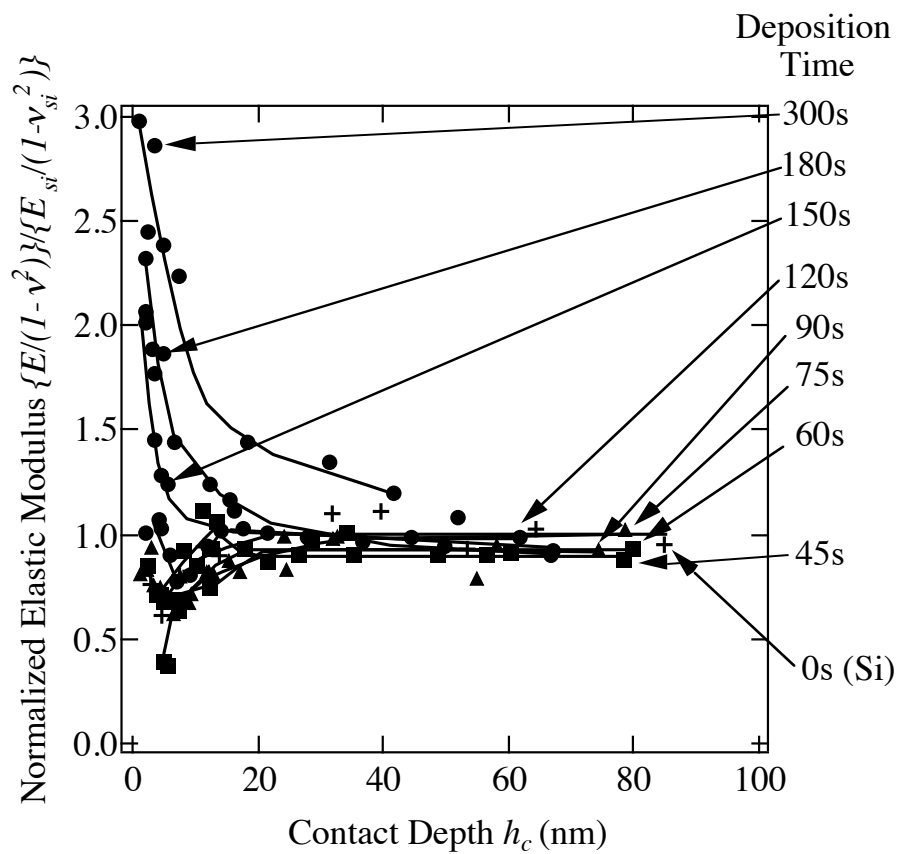


Figure 4 (a)

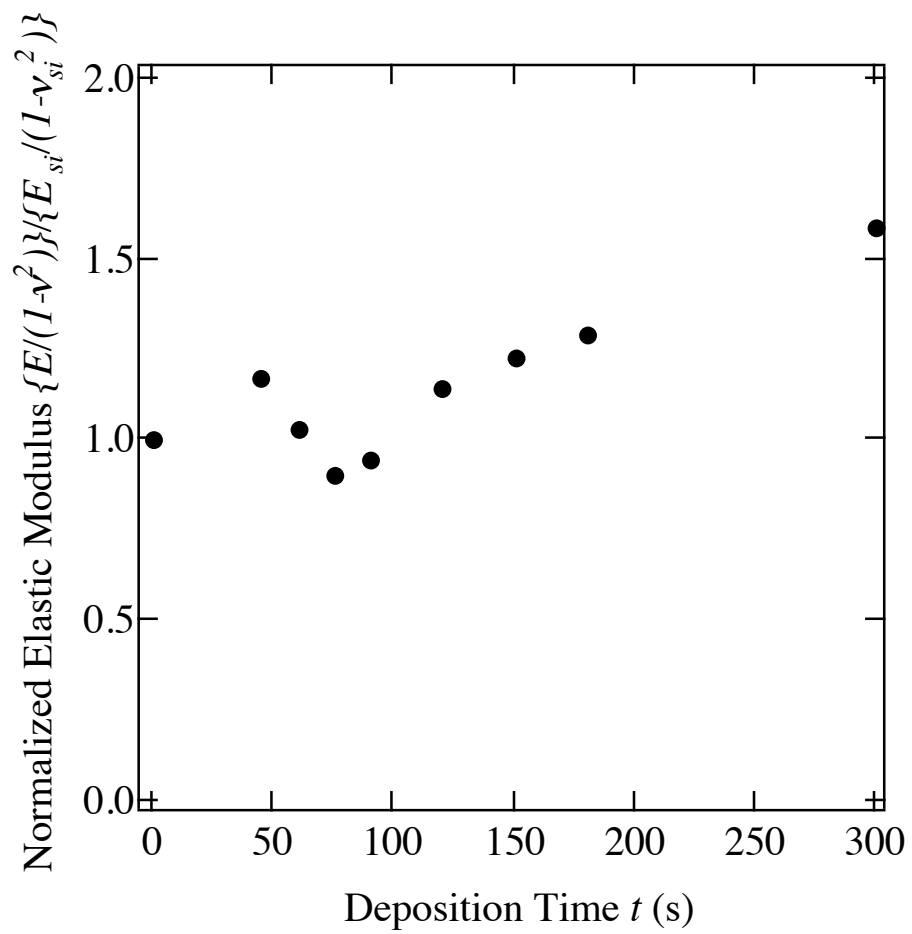


Figure 4 (b)